

Motion Control of Linear Permanent Magnet Motors with Force Ripple Compensation

Röhrig, Christof

Department of Electrical Engineering and Information Technology
University of Hagen
Feithstr. 140, D-58097 Hagen, Germany
Phone: +49-2331-987-1102, Fax: +49-2331-987-354
E-Mail: christof.roehrig@fernuni-hagen.de

Jochheim, Andreas

Hesse & Knipps GmbH

Abstract

The main problem in improving the tracking performance of linear permanent magnet motors is the presence of force ripple caused by the irregular magnetic field of the permanent magnets and inaccuracy in electronic commutation by the servo amplifier. In this paper a motion controller with force ripple compensation is presented. A physical model of the linear motor and the force ripple is derived first. The controller design based on a Fourier series approximation to compensate the effect of the force ripple. A comparison of the tracking performance with and without ripple compensation is given.

Key words: motion control, force ripple, linearization.

1 Introduction

Linear permanent magnet motors are beginning to find widespread industrial applications, particularly for tasks requiring a high precision in positioning such as various semiconductor fabrication and inspection processes [1]. Other possible applications are high speed and high productivity NC machine tools [2]. Linear permanent magnet motors appear to have a significant application potential for a wide range of industrial applications [3]. The main benefits of linear motors are the high force density achievable and the high positioning precision and accuracy associated with the mechanical simplicity of such systems. The electromagnetic force is applied directly to the payload without any mechanical transmission such as chains or screw couplings. This greatly reduces nonlinearities and disturbances caused by backlash and additional frictional forces [4]. The more predominant nonlinear effects underlying a linear motor system are friction and force ripples arising from imperfections in the underlying components e.g. irregular magnetic field, inaccuracy of commutation. In order to avoid force ripple different methods have been developed. The arrangement of the permanent magnets can be optimized to reduce cogging forces [5],[6]. In [7] a force ripple model is developed and identification is carried out with a force sensor and a frictionless air bearing support of the motor carriage. In [8] a neuronal-network based feedforward

controller is proposed to reduce the effect of force ripple. Position-triggered repetitive control is presented in [9]. Other approaches are based on disturbance observers [10], [11], iterative learning control [12] or adaptive control [13]. In this paper a model based approach is proposed, because force ripple is a highly reproducible and time-invariant disturbance. The force ripple model is based on a Fourier series approximation and is identified by measuring the control signal in a closed position control loop for different load forces. The model considers both, current-dependent and current-independent force ripple. The paper is organized as follows: In Section 2 the experimental setup is described. In Section 3, a physical model of the linear motor is derived and explained. The identification of the model parameters is presented. In Section 4 the controller design is presented and a comparison of the tracking performance with and without ripple compensation is given. Finally Section 5 concludes the paper.

2 Experimental Setup

The motors considered here are brushless permanent magnet linear motors with epoxy cores. A linear motor consists on a stator and a moving translator (counterpart of the rotor in a rotating motor). There are two basic classifications of permanent magnet servo motors: epoxy core (i.e. non-ferrous, slotless) and steel core. Epoxy core motors have coils wound within epoxy support. This motors have a closed magnetic path through the gap since two magnetic plates "sandwich" the coil assembly [14]. Figure 1 shows an unmounted brushless permanent magnet linear motor. The stator induces a multipole magnetic field in the air gap between the magnetic plates. The magnet assembly consists of rare earth magnets, mounted in alternate polarity on the steel plates. The electromagnetic thrust force is produced by the interaction between the permanent magnetic field in the stator and the magnetic field in the translator driven by the current of the servo amplifier. The linear motors under evaluation are current-controlled three-phase motors driving carriages supported by roller bearings. The commutation of the three phases is done electronically in the power amplifier.

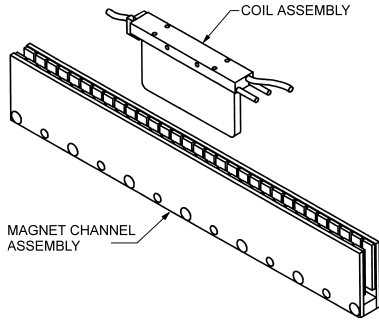


Figure 1. Anorad LE linear motor [14]

In the experimental setup two different linear motors (LEA-S-4-S and LEM-S-4-S) are used. Figure 2 shows the Y-axis driven by the LEA-S-4-S linear motor.

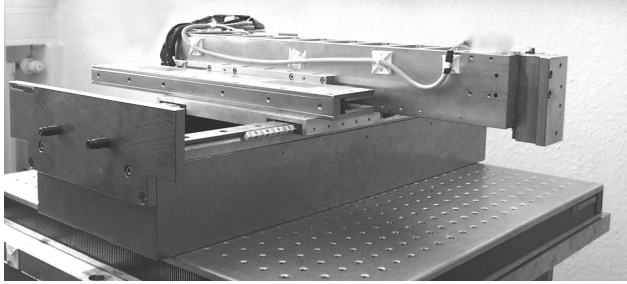


Figure 2. Experimental setup

The servo amplifiers used in the setup are PWM types with closed current control loop. The commutation is done with the help of the position encoder or with hall sensors [15], [16]. The dynamics of the servo amplifier will not be considered as they play a minor role in the dynamics of the whole system.

3 System Modeling

Two types of position dependent disturbances are considered: cogging force and force ripple. Cogging is a magnetic disturbance force that is caused by attraction between permanent magnets and translator. The force depends on the relative position of the translator with respect to the magnets, and it is independent of the motor current. Force ripple is an electro-magnetic effect and causes a periodic variation of the force constant c_ϕ . Force ripple occurs only if the motor current is different from zero, and its absolute value depends on the required thrust force and the relative position of the translator to the stator. Both disturbances are periodic functions of the position. [9]

Cogging is negligible in motors with iron-less translators [14]. Figure 3 shows the nonlinear block diagram of a servo system with brushless linear motor. The nonlinear

disturbances are the velocity depended friction force $F_{friction}$, and the position dependent cogging force $F_{cogging}$ and force ripple $c_\phi(x)$.

The friction force is modeled with a kinetic friction model. In the kinetic friction model the friction force is a function of velocity only. The friction curve is identified with experiments at different velocities. The friction has a discontinuity at $\dot{x} = 0$, because of stiction. Stiction avoid accurate measurement of the thrust force without motion of the carriage. A survey of friction models and compensation methods is given in [17].

Aim of the force ripple identification is to obtain a function of the thrust force F_{thrust} versus the control signal u and the position x . A possible solution to identify this function is to measure the thrust force F_{thrust} at different positions x and control signals u . In this case an additional force sensor and a screw cylinder for manual position adjustment is necessary. In order to measure the force ripple accurately, without motion of the carriage, a frictionless air bearing support is necessary [7]. A solution to avoid frictionless air bearings is the measurement of the thrust force with moving carriage. At constant velocities the friction force is also constant and can be treated as additional load force. In this case an additional servo system is needed to achieve the movement [18].

The main idea of the proposed identification method is to identify the force ripple in a closed position control loop by measuring the control signal u at different load forces F_{load} and positions x . Neither additional force sensor nor device for position adjustment are necessary. In order to avoid inaccuracy by stiction the measurement is achieved with moving carriage. The position of the carriage is obtained from an incremental linear optical encoder with a measurement resolution of $0.2\mu m$. The experiment consists of several movements at constant low velocity ($1mm/s$) and different load forces ($0 \dots 70N$). The output of the position controller is stored at equidistant positions. A controller with an integral component is used to eliminate steady position error. During motion with constant low velocity the dynamics of the motor have no significant effect on the control signal u .

Figure 4 shows the controller output u versus the translator position x . In this first experiment there is no additional load force attached to the carriage. The period spectrum of the controller signal u_i is carried out via FFT.

$$u_i = f(x_i) = \frac{1}{N} \sum_{k=0}^{N-1} c_k e^{j2\pi k \frac{x_i}{L}} \quad (1)$$

$$x_i = x_0 + i \frac{L}{N}, i = 0 \dots N - 1 \quad (2)$$

$$c_k = \sum_{i=0}^{N-1} u_i e^{-j2\pi k \frac{x_i}{L}} \quad (3)$$

Where L is the length of the movement, N is the number of measured signals and c_k are the complex

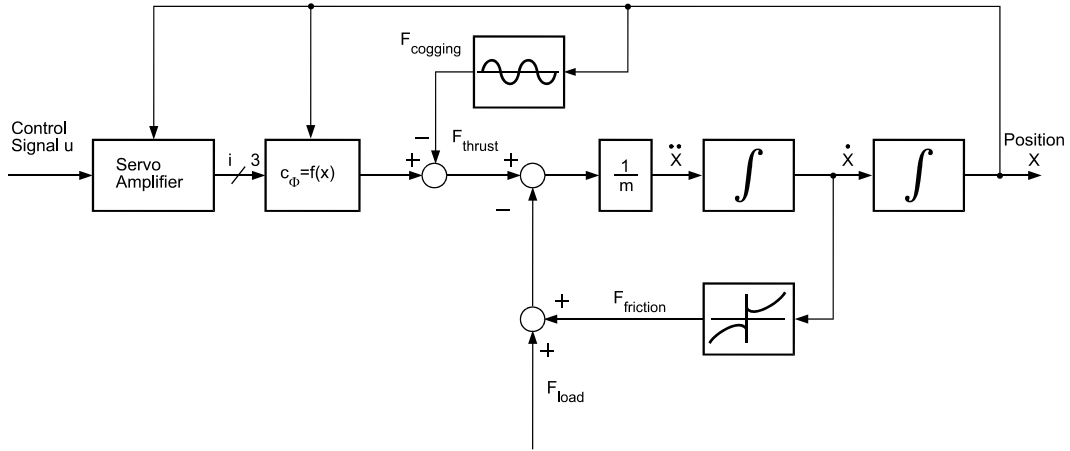


Figure 3. Nonlinear model of a brushless linear motor

discrete Fourier coefficients.

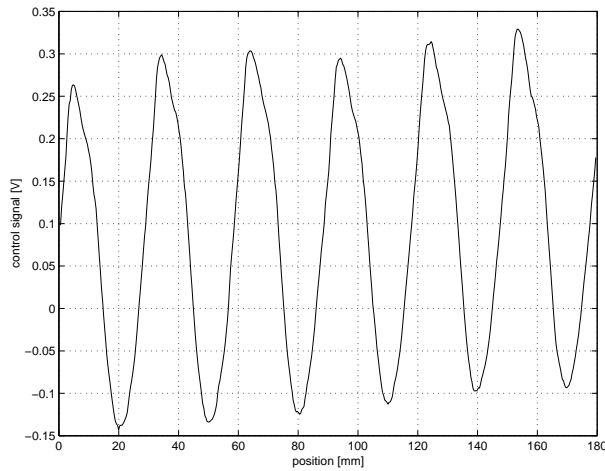


Figure 4. Force ripple without additional load force

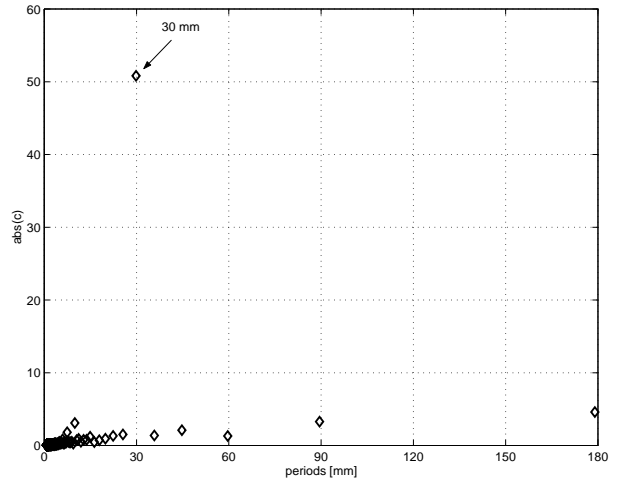


Figure 5. Spectrum of force ripple without additional load force

Figures 5 and 7 display absolute values of the Fourier coefficients $|c_k|$ as rhombuses versus corresponding discrete periods L/k . Figure 5 shows the period spectrum of the experiment without additional load force. The fundamental period (30mm) corresponds to the distance between two permanent magnets with the same polarity in the stator. Figure 6 displays the controller signal with an additional load force of 70N . The spectrum in figure 7 indicates two additional harmonics at 15mm and 7.5mm . The sinusoid with the period of 30mm appears at the same level as the experiment without additional load force. This current-independent ripple is measured even though the translator is build without iron. At heavy load forces the current-dependent force ripple prevails the current-independent ripple. Force ripple can be modeled as a sinusoid with higher order harmonics. The force ripple is complex in shape e.g., due to variations in the magnetic field of the stator. It is a periodic function and can be approximated with a Fourier series. The

numerical analysis of the measured data was done with MATLABTM. The discrete Fourier Transformation has the disadvantage that only periods for whole-numbered divisors of the measured movement can be detected. In order to determine the period more exactly, the data-fitting optimization of MATLABTM was applied on function (4).

$$f(x) = c_1 + c_2 x + \sum_{k=0}^{M-1} c_{2k+4} \sin\left(\frac{2\pi(k+1)}{c_3}(x + c_{2k+5})\right) \quad (4)$$

The physical meaning of the parameter vector \mathbf{c} of function (4) is: c_1 is the average of the controller signal (desired thrust force), c_2 is the gradient of the curve e.g. caused by sealing bellows, c_3 is the highest dominant period, c_{2k+4} are the amplitudes of the sinusoids, c_{2k+5} are the phase shifts of the sinusoids and M is the number of detected sinusoids with spectrum analysis.

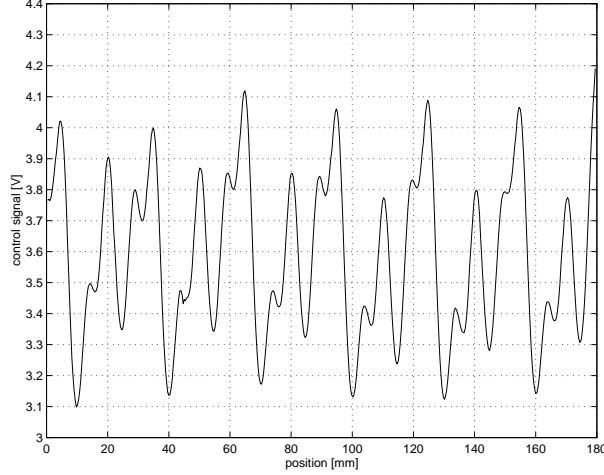


Figure 6. Force ripple at load force $F = 70$ N

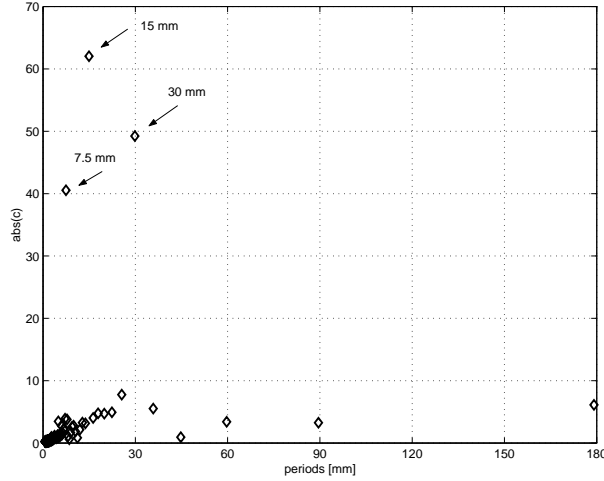


Figure 7. Spectrum of force ripple at load force $F = 70$ N

The minimization (5) is done with the N measured controller signals u_i at positions x_i . The result of the minimization is a parameter vector \mathbf{c} of model function (4) that best fits the measured curve.

$$\min_{\mathbf{c}} \sum_{i=0}^N (f(x_i, \mathbf{c}) - u_i)^2 \quad (5)$$

The nonlinear least square algorithm of MATLAB™ uses the "large-scale algorithm" based on the "interior-reflective Newton method" for optimization of the vector \mathbf{c} [19]. The initial values of \mathbf{c} are taken from the previous spectrum analyses. An identification procedure was written in the MATLAB™ scripting language. The procedure does the optimization of \mathbf{c} with data of experiments at different load forces. It detects whether the amplitudes c_{2k+4} depend on the load force ($\sim c_1$) or not. The result of the identification procedure are the parameters of function (6) to compensate the effect of the

force ripple.

$$u(x, u') = \alpha(x) + \beta(x) u' \quad (6)$$

$$\alpha(x) = k_c x + \sum_{k=1}^M a_k \sin\left(\frac{2\pi k}{\lambda_0} (x + c_k)\right) \quad (7)$$

$$\beta(x) = 1 + \sum_{k=1}^N b_k \sin\left(\frac{2\pi k}{\lambda_1} (x + d_k)\right) \quad (8)$$

Where M is the number of current-independent sinusoids, N is the number of current-dependent sinusoids, x is the position of carriage, u' is the controller output (desired thrust force), u is the servo amplifier input, k_c is the gradient of the curve e.g. caused by sealing bellows, a_k are the current-independent amplitudes, b_k are the current-dependent amplitudes, c_k , d_k are the phase shifts and λ_0 , λ_1 are the periods.

In Figure 8 a comparison of the model and the measured control signal is shown. The carriage was loaded with a negative force. The differences between the curves are caused by inaccuracies of position and dimension for individual magnets. The model assumes perfect periodicity of the ripple force.

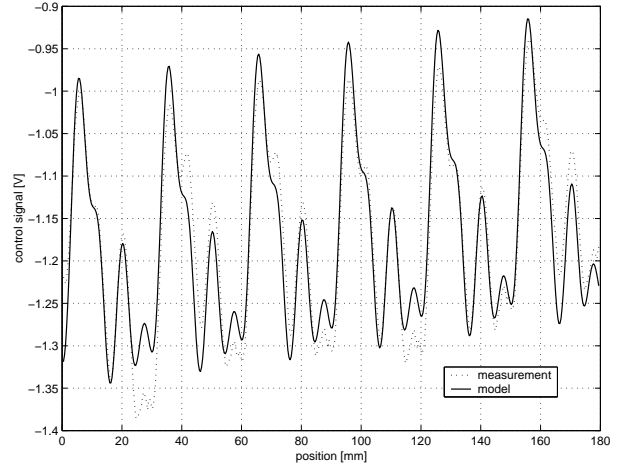


Figure 8. Comparison of model and measurement

4 Controller Design

Figure 9 shows the block diagram of the servo control system. In order to achieve a better tracking performance, a feedforward controller is applied. Feedback control without feedforward control always introduces a phase lag in the command response. Feedforward control sends an additional output, besides the feedback output, to drive the servo amplifier input to desired thrust force. The feedforward control compensates the effect of the carriage mass and the friction force. The friction force

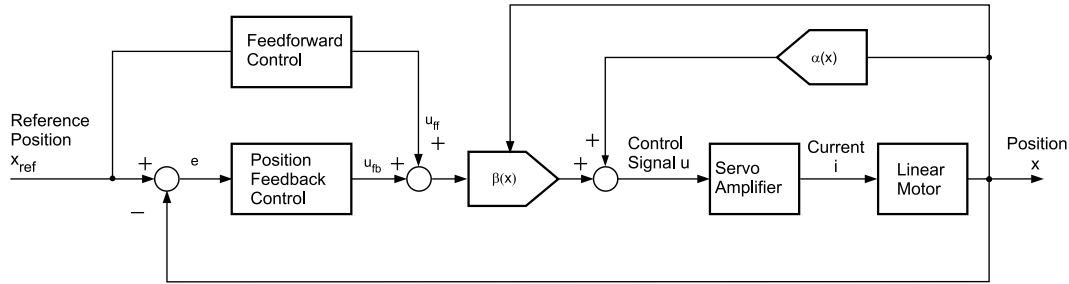


Figure 9. Force ripple compensation

is modeled by a kinetic friction model and identified with experiments at different velocities. The mass of the carriage is identified with a dynamic least square algorithm. The stability of the system is determined by the feedback loop. Feedback linearization of friction with the kinetic friction model has been proposed in numerous literature references, but is rarely applied successfully because undesirable oscillations result easily from this approach [20]. The compensation of the force ripple is applied with input-output linearization. The function $\beta(x)$ compensates the effect of the current-dependent ripple the function $\alpha(x)$ the effect of current-independent ripple. Figure 10 compares the tracking error of a movement without ripple compensation with the movement with ripple compensation. In this measurement, the carriage moves from position 50mm to position 150mm and back to position 50mm with $v_{max} = 200\text{mm/s}$. If the ripple compensation is applied, the tracking error is reduced significantly. Figure 11 shows the control signal u and the output of the feedforward controller with force ripple compensation. The difference between the signals are caused by model inaccuracies.

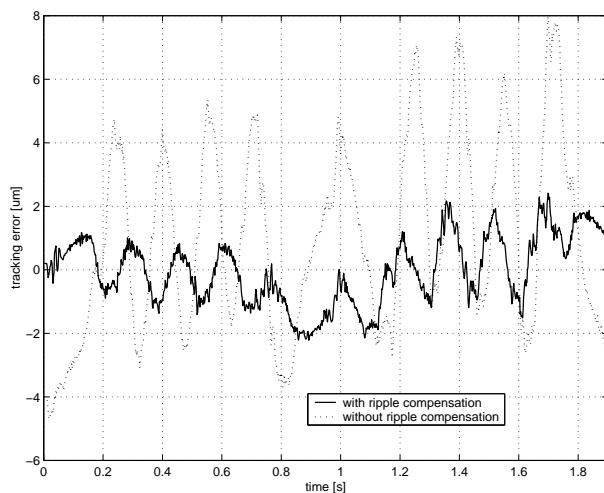


Figure 10. Tracking error

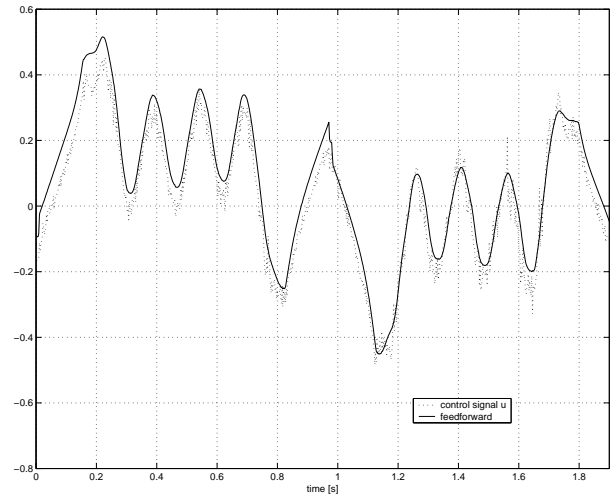


Figure 11. Controller Signals

5 Conclusion

In this paper, a motion controller with force ripple compensation is presented. The force ripple model is based on Fourier series approximation of the periodic ripple function. In order to identify the model parameters, no additional sensors are required. The model was identified with non-iron-coil permanent magnet motors. Since it considers current-independent ripple, it can also be applied on iron-coil permanent magnet motors. Experiments show that the tracking performance is significantly improved if the ripple compensation is applied.

References

- [1] A. Basak. *Permanent-Magnet DC Linear Motors*. Clarendon Press, Oxford, 1996.
- [2] Y. Kakino. Tools for High Speed and High Acceleration Feed Drive System of NC Machine Tools. In *Proceedings of the 2th International Symposium on Linear Drives for Industry Applications*, pages 15–21, Tokyo, Japan, April 1998.

- [3] D. Howe and Z. Q. Zhu. Status of Linear Permanent Magnet and Reluctance Drives in Europe. In *Proceedings of the 2th International Symposium on Linear Drives for Industry Applications*, pages 1–8, Tokyo, Japan, April 1998.
- [4] G. Pritschow. A Comparison of Linear and Conventional Electromechanical Drives. *Annals of the CIRP*, 47(2):541–548, 1998.
- [5] I.S. Jung, J. Hur, and D.S. Hyun. 3-D Analysis of Permanent Magnet Linear Synchronous Motor with Magnet Arrangement Using Equivalent Magnetic Circuit Network Method. *IEEE Transactions on Magnetics*, 35(5):3736–3738, September 1999.
- [6] R.J. Cruise and C.F. Landy. Reduction of Detent Forces in Linear Synchronous Motors. In *Proceedings of the 2th International Symposium on Linear Drives for Industry Applications*, pages 412–415, Tokyo, Japan, April 1998.
- [7] P. Van den Braembussche, J. Swevers, H. Van Brussel, and P. Vanherck. Accurate Tracking Control of Linear Synchronous Motor Machine Tool Axes. *Mechatronics*, 6(5):507–521, 1996.
- [8] G. Otten, T.J.A. de Vries, J. van Amerongen, A.M. Rankers, and E.W. Gaal. Linear Motor Motion Control Using a Learning Feedforward Controller. *IEEE/ASME Transactions on Mechatronics*, 2(3):179–187, 1997.
- [9] P. Van den Braembussche, J. Swevers, and H. Van Brussel. Linear Motor Ripple Compensation Using Position-triggered Repetitive Control. In *Proceedings of the IFAC Workshop on Motion Control*, pages 353–357, Grenoble, France, 1998.
- [10] E. Schrijver and J. van Dijk. H_∞ Design of Disturbance Compensators for Cogging Forces in a Linear Permanent Magnet Motor. *Journal A*, 40(4):36–41, 1999.
- [11] F.J. Lin, C.H. Lin, and C.M. Hong. Robust Control of Linear Synchronous Motor Servodrive Using Disturbance Observer and Recurrent Neural Network Compensator. *IEE Proceedings Electric Power Applications*, 147(4):263–272, 2000.
- [12] T.H. Lee, K.K. Tan, S.Y. Lim, and H.F. Dou. Iterative Learning of Permanent Magnet Linear Motor with Relay Automatic Tuning. *Mechatronic*, 10(1-2):169–190, 2000.
- [13] L. Xu and B. Yao. Adaptive Robust Precision Motion Control of Linear Motors with Ripple Force Compensations: Theory and Experiments. In *Proceedings of the IEEE Conference on Control Applications*, pages 373–378, September 2000.
- [14] Anorad Corporation. *LE Series Linear Motor Systems, Motor Integration Manual LEA, LEB, LEC & LEM Linear Motors*, September 1999.
- [15] Glentek. *Operation & Installation Manual for Model SMA9715 Brushless Digital Amplifier System*, January 2001.
- [16] Anorad Corporation. *High Voltage Brushless D.C. Servo Amplifier, Hardware Maintenance Manual*, February 1998.
- [17] B. Armstrong-Hélouvry, P. Dupont, and C. Canudas de Wit. A Survey of Models, Analysis Tools and Compensation Methods for the Control of Machines with Friction. *Automatica*, 30(7):1083–1138, 1994.
- [18] U. Brahms. *Regelung von Lineardirektantrieben für Werkzeugmaschinen*. PhD thesis, Universität Hannover, 1998. VDI-Verlag, Reihe 8, Nr. 735.
- [19] The Mathworks Inc. *Optimization Toolbox User's Guide*, 1999.
- [20] F. Altpeter. *Friction Modeling, Identification and Compensation*. PhD thesis, École Polytechnique Fédérale de Lausanne, 1999.